Strength of Materials, Vol. 26, No. 4, 1994

NUMERICAL METHOD FOR OPTIMIZING THE DESIGN OF A HIGH-PRESSURE APPARATUS WITH DIAMOND ANVILS

N. V. Novikov, V. I. Levitas, S. B. Polotnyak, and M. M. Potemkin

UDC 539.374

A numerical method for optimizing the structure of a high-pressure unit with diamond anvils as pressure is created in the vessel is developed and realized in the form of a set of programs. The method includes the following: determination of the stress–strain state of the anvils and the deformable intervening layer of material; evaluation of the strength of the anvils; the development of a mathematical model to describe the dependence of the strength of the anvils on the parameters being optimized; determination of the optimum points of the model. A combination of optimum parameters is obtained, making it possible to reach a design pressure of 465 GPa. This pressure is 2.5 times higher than the pressure recorded in anvils with a similar pressure distribution (N. K. Mao and P. M. Bell, 1978).

The use of diamonds as anvils in high-pressure units (HPU) makes it possible to conduct a broad spectrum of physicomechanical investigations at static pressures in the megabar range [1]. Pressure in such units is generated during the compression of a deformable interlayer (DI) between the small flat ends of two oppositely positioned cut gem diamonds. One way of increasing the maximum pressure attainable in such units is to improve the stress–strain state of the anvils by altering their geometry and loading conditions. This problem can be approached either experimentally or theoretically. The first, more traditional approach entails considerable material costs, since one or both anvils are damaged during compression (unloading). The second, theoretical approach involves constructing a mathematical model to describe the behavior of the main elements of an HPU and then optimizing the parameters that go into the model.

Several attempts have been made to analyze the stress–strain state (SSS) of diamond anvils [2-8]. In particular, the study [2] examined the main principles underlying the design of an HPU for obtaining megabar pressures. Requirements regarding the geometry and constituent materials of an HPU were also set forth in [2]. In [3-5], a finite-element analysis was made of the stress–strain state of diamond anvils within the framework of the theory of elasticity of isotropic bodies. The authors analyzed several variants of model loads and obtained distributions of the principal σ_1, σ_2 and octahedral shear τ_{oct} stresses in anvils. The bevel angle of the working surface $\alpha = 15°$ was established on the basis of the lowest maximum stresses τ_{oct}. The strength of anvils was evaluated in [5] using the Pisarenko–Levedev criterion, and an analysis was made of the main mechanisms by which anvils fail. Approximate methods were employed in [6, 7] to calculate the pressure corresponding to the beginning of plastic flow in a single crystal of perfect diamond ($\sigma_y \approx 960$ GPa). An analysis of the stress–strain state of the anvils and the intervening layer in an HPU in [8] led the authors to doubly truncate the working surface.

In the present study, we resort to numerical optimization of the geometry of diamond anvils and the conditions of their loading to accomplish the following: determine the limiting state of the DI; calculate the stress–strain state and strength of the anvils; construct a mathematical model to describe the dependence of the strength of the anvils on their geometry and loading conditions; find the optimum points of the model for the a maximum of generated pressure.

To establish the critical state of the interlayer (which undergoes compression between the elastic diamond anvils), we propose to use a theoretical–empirical method which involves evaluation of the plastic constants of the material of the interlayer and the lateral pressures on it. The method also entails the numerical solution of the problem of the compression of a thin disk between two elastic diamond anvils.

The constants K and ρ of the material of the interlayer, entering into the Coulomb yield condition

$$\tau_n = K + \sigma_n \operatorname{tg} \rho \qquad (1)$$

Institute of Ultrahard Materials, Ukrainian Academy of Sciences, Kiev. Translated from Problemy Prochnosti, No. 4, pp. 64-74, April, 1994. Original article submitted July 27, 1992.

0039-2316/94/2604-0294$12.50

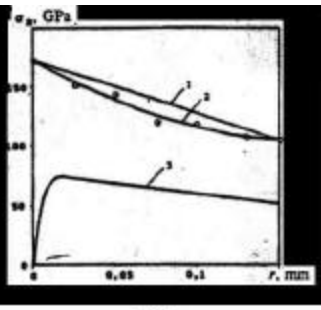

Fig. 1

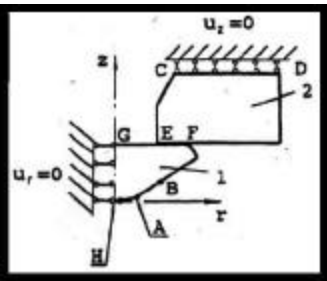

Fig. 2

Fig. 1. Stress distribution along the line of contact of a diamond anvil and the interlayer: 1 and 2) normal stresses σ_n at $\rho = 0$ and 10^{-4}, respectively; 3) shear stresses τ_n. (The points show data from [9]).

Fig. 2. Theoretical scheme used to determine the stress–strain state of diamond anvils: 1) diamond anvil; 2) hard-alloy support.

(σ_n and τ_n being the normal and tangential pressures on the slip plane, K the shear strength at $\sigma_n = 0$, and ρ the angle of internal friction), were determined from an analysis of experimental data [9] on the radial distribution of pressure $\sigma_0(r)$ for an interlayer made of quenched stainless steel T301 compressed by a factor of 40 between diamond anvils (Fig. 1). We will use the simplified equilibrium equation [10]

$$\frac{d\sigma_0}{dr} = -\frac{2\tau_s(\sigma_0)}{h(r)}, \quad (2)$$

where $\tau_s(\sigma_0)$ is the dependence of shear strength on hydrostatic pressure (represented for most materials in the form $\tau_s = K_1 + \sigma_0 \tan\rho_1$); h(r) is the thickness of the interlayer; r is the running radius of points of the contact surface; $K_1 = K[\cos^2\rho/(1 - 1/3\sin\rho)]$; $\tan\rho_1 = \tan\rho[\cos^2\rho/(1 - 1/3\sin\rho)]$ [11]. Differentiating the graph of $\sigma_0(r)$ and multiplying the result by $(-h(r)/2)$, we obtain the relation $\tau_s(\sigma_0)$ and use the latter to find K_1, ρ_1 and, accordingly, K = 2.22 GPa, ρ = 0.00015. To check this result, we integrate (2) and, having inserted K_1 and ρ_1 into it, we find the theoretical distribution of $\sigma_0(r)$. This distribution is then compared with the empirical distribution.

According to [9], the distribution of the normal stresses σ_n supporting the sides of the die can be described by an exponential law. The jump in σ_n at point A (Fig. 2) is due to the geometry of the dies and is evaluated as $2K(\theta_1 - \alpha)$ [12], where θ_1 is the angle between the lateral surface of the die and the horizontal plane. The magnitude of the jump in σ_n at point B is $K(1 + 2(\pi/2 - \theta_1))$. The lateral shear stresses are assumed to conform to distribution (1).

The critical state of the interlayer was calculated numerically by the slip-line method. Since the strains of the material of the layer are large and since the loading is monotonic, we used the model of an ideally plastic isotropic and uniform material [11]. The problem will be solved in an axisymmetric formulation. The closed system of equations for solving the problem includes:

the equilibrium equations

$$\sigma_{ij,j} + F_i = 0; \quad (3)$$

the equation of the limit surface corresponding to ideal plasticity (1);
the condition of complete plasticity

$$\sigma_3 = \sigma_2, \quad (4)$$

where σ_{ij} are components of the stress tensor (σ_r, σ_z, σ_θ, and τ_{rz} in a cylindrical coordinate system); σ_2 and σ_3 are the principal stresses.

We used the "Plastic Deformation" application package [11] to solve the problem. The values obtained for K and ρ are used as the initial data for subsequent iterative approximation of the empirical distribution of contact stresses. We finally obtain K = 2.24 GPa, $\rho = 10^{-4}$. Despite the small value of ρ, a significantly greater difference is obtained between the theoretical and experimental results (Fig. 1) if we assume that $\rho = 0$.

The calculation gave us distributions of the components σ_{ij} in the interlayer (directly under the anvils) and normal σ_n and shear τ_n stresses on the working surface of the anvils (Fig. 1). This information was then used to formulate boundary conditions for evaluation of the stress–strain state of the anvils. We should point out the presence of the large gradient in σ_n over the working surface.

The application package "Elasticity-2" was developed [13] to determine the stress–strain state of diamond anvils. These programs employ the finite-element method together with a set of isoperimetric elements [13]. Testing of the package (using sample problems and the method described in [14]) showed that the results obtained are satisfactory. There are three independent elastic constants – C_{11}, C_{12}, C_{44} – for cubic crystals (including diamond). In a crystallographic coordinate system, Hooke's law for diamond has the form $\sigma = [C]\varepsilon$, where σ and ε are the stress and strain tensors, respectively; [C] is the matrix of elastic constants [15]. Since the anvils are nearly conical and since the distribution of contact stresses over their surface is axisymmetric, the problem is solved in an axisymmetric formulation within the framework of the theory of elasticity of anisotropic bodies. The axis of symmetry z of the cylindrical coordinate system coincides with the axis of rotation and the ⟨001⟩ direction in the diamond crystal.

A standard procedure [16] is used to transform the components of the matrix [C] of the diamond from the crystallographic coordinate system to the cylindrical system. Averaging the values obtained for the elastic coefficients over the angle θ and taking $\tau_{z\theta}$ and $\tau_{r\theta}$ equal to zero, we write Hooke's law as follows for the case of axisymmetric deformation of a transversely isotropic body of rotation:

$$\begin{Bmatrix} \sigma_r \\ \sigma_z \\ \sigma_\theta \\ \tau_{rz} \end{Bmatrix} = \begin{bmatrix} B_{11} & B_{12} & B_{13} & 0 \\ B_{12} & B_{11} & B_{13} & 0 \\ B_{13} & B_{13} & B_{33} & 0 \\ 0 & 0 & 0 & B_{44} \end{bmatrix} \begin{Bmatrix} \varepsilon_r \\ \varepsilon_z \\ \varepsilon_\theta \\ 2\varepsilon_{rz} \end{Bmatrix}$$

where ε_{rr}, ε_{zz}, $\varepsilon_{\theta\theta}$, ε_{rz} are components of the strain tensor; $B_{11} = C_{11} + \frac{1}{4}(C_{12} - C_{11} + 2C_{44})$; $B_{12} = C_{12} + \frac{1}{4}(C_{11} - C_{12} - 2C_{44})$; $B_{13} = C_{12}$; $B_{33} = C_{11}$; $B_{44} = C_{44}$.

Figure 3 shows the boundary conditions and theoretical scheme employed to solve the problem. We assigned the following boundary conditions: along line CD – absence of displacements in the direction of the z axis $u_z = 0$ and $\tau_n = 0$; along line EF – ideal bonding of the materials of the anvil and the supporting insert; along line GH – $u_r = 0$ and $\tau_n = 0$; along line HA – distribution of the contact σ_n and τ_n stresses (Fig. 1); along line AB – distribution of the lateral stresses σ_n and τ_n; on the remaining surfaces $\sigma_n = \tau_n = 0$. The properties of the materials: diamond – C_{11} = 1076 GPa; C_{12} = 126 GPa; C_{44} = 548 GPa; the hard-alloy support – elastic modulus E = 640 GPa, Poisson's ratio ν = 0.22. Having completed the finite-element calculations, we obtain the fields of σ and ε in the diamond anvils (Fig. 3a). Figure 3b shows isolines of components of the stress tensor in the case when the elastic properties are not anisotropic. A comparison showed that ignoring the effect of anisotropy produces an error of more than 10% in the determination of the maximum stresses in the anvils. The highest compressive and shear stresses occur near the working boundary of the anvil. The maximum tensile stresses σ_r and σ_θ develop at the base of the anvil under the unsupported hole made in the structure to admit light (section GE in Fig. 2). These maxima are is near the working surface on the axis of symmetry.

An analysis of fractured single crystals of diamond established [15] that this is an extremely brittle material which fractures along cleavage planes due to the presence of tensile stresses from the nucleation and growth of microcracks. Fracture in this case usually occurs earlier than fracture due to plastic deformation. Thus, the region in which tensile stresses are greatest will pose the most danger to the material. In order to evaluate the strength of the anvils, it is necessary to find a criterion that adequately describes the brittle fracture of materials with the structure of diamond while accounting for the anisotropy of its strength characteristics and requiring a minimum amount of experimental data. For brittle anisotropic materials that fracture by brittle rupture along certain planes, it is usually assumed that the normal tensile stresses σ_n – which depend on the orientation of the fracture plane – reach critical values [17]. However, this criterion does not describe the fracture in diamond anvils in nonequilibrium triaxial compression. Thus, it was proposed in [18] that the

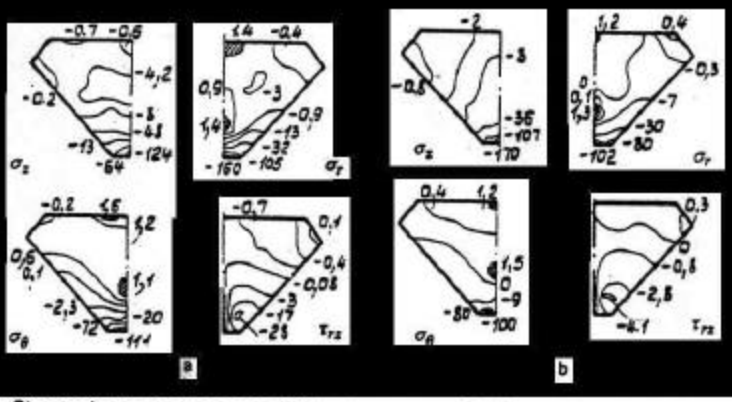

Fig. 3. Change in the components of the stress tensor in diamond anvils during loading with (a) and without (b) allowance for the anisotropy of the elastic properties.

effect of the components of the stress tensor other than σ_n be accounted for within the framework of the model of a medium which undergoes structural changes. In a special case, it follows from this approach that the criterion of maximum extension in cleavage planes is valid and best describes the limiting state of diamond [19]:

$$\sigma_e = \varepsilon^{\max}_{<ijk>} E_{<ijk>} = \sigma^0_{<ijk>}, \tag{5}$$

where $\varepsilon^{max}_{(ijk)}$ is the maximum strain in the directions perpendicular to the planes (ijk) along which the crystal fractures under the given type of loading; $E_{(ijk)}$ is the elastic modulus in the direction (ijk); $\sigma^0_{(ijk)}$ is ultimate strength in the case of cleavage along these planes. However, use of the above criterion requires experimental determination of σ^0 for each of the cleavage planes under consideration. It is proposed that the amount of experimental data needed be reduced by using a well-known theoretical relation that was substantiated experimentally in [15] and expresses the dependence of ultimate tensile strength ($\sigma_1 > 0$, $\sigma_2 = \sigma_3 = 0$) on the Miller indices of the slip plane [20]:

$$\sigma_1 = \sqrt{2\gamma_{(ijk)}E^*/\pi(1-\nu^*)^2 C_f}, \quad \gamma_{(ijk)} = \sqrt{3}\gamma_{(111)}\frac{|i|}{(i^2+j^2+k^2)^{1/2}} \text{ [21]}, \tag{6}$$

where $\gamma_{(ijk)}$ is the surface energy for the fracture plane (ijk); E^* and ν^* are the averaged elastic modulus and Poisson's ratio, $E^* = 1138$ GPa, $\nu^* = 0.072$ [15]; C_f is the average size of the microcrack-type defects initially present. Inserting the conditions $\sigma_1 \neq 0$, $\sigma_2 = \sigma_3 = 0$ into Eq. (5), we obtain the following for the local coordinate system connected with the fracture plane (ijk).

$$\sigma_1 = \sigma^0_{<ijk>} \tag{7}$$

Having inserted (7) into (6), we write the final expression for the strength criterion for diamond. It contains only one constant:

$$\sigma_e = \varepsilon^{\max}_{<ijk>} E_{<ijk>} = m\left(\frac{|i|}{(i^2+j^2+k^2)^{1/2}}\right)^{1/2} = \sigma^0_{<ijk>}, \tag{8}$$

where

$$m = \sqrt{2\sqrt{3}\gamma_{(111)}E^*/\pi C_f}.$$

To determine m, we experimentally find the ultimate strength for one fracture plane – say $[pln]$. Then

$$m = \sigma^0_{<pln>} / \left(\frac{|p|}{(p^2+l^2+n^2)^{1/2}}\right)^{1/2}. \tag{9}$$

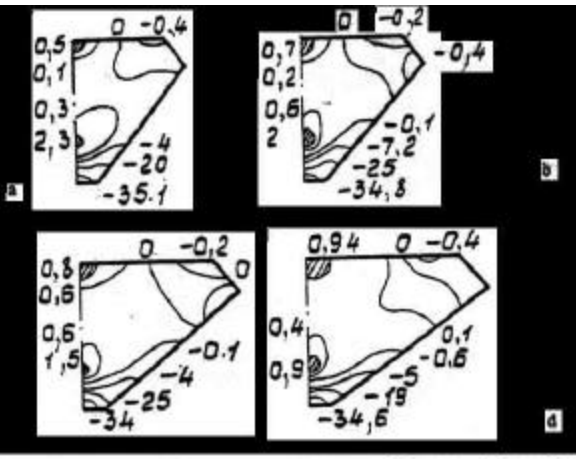

Fig. 4. Distribution of isolines of corrected equivalent stress $\sigma_e/\sigma^0_{\langle 110\rangle}$ in diamond anvils with a ratio of the height of the anvil to the diameter of its base H/D equal to 1:1 (a); 2:3 (b); 1.2 (c); 1:3 (d).

It is known [15] that (110) and $(1\bar{1}0)$ will be the most probable fracture planes when a single crystal of diamond is compressed in the direction ⟨001⟩. The strains $\varepsilon_{(110)}$, $\varepsilon_{(1\bar{1}0)}$ and elastic moduli $E_{(110)}$, $E_{(1\bar{1}0)}$ in a cylindrical coordinate system $r\theta z$ are connected with the components of the strain tensor and elastic constants by the following expressions [22]:

$$\varepsilon_{\langle 110\rangle} = \varepsilon_r;\ \varepsilon_{\langle \bar{1}10\rangle} = \varepsilon_\theta;\ E_{\langle 110\rangle} = E_{\langle \bar{1}10\rangle} = C_{11} + \frac{1}{4}(C_{12} - C_{11} + 2C_{44}).$$

According to the data in [19], the ultimate strength of diamond undergoing cleavage along the (110) and $(1\bar{1}0)$ planes is 2.67 GPa. We thus find from (9) that m = 3.175. This value of strength corresponds to the following size of the microcracks on the surface of diamond

$$C_f = \frac{2\gamma_{(110)}E^*}{\pi(1-\nu^*)^2(\sigma_{\langle 110\rangle})^2} = 7{,}67\cdot 10^{-5}\ \text{см},$$

where $\gamma_{(110)} = \gamma_{(1\bar{1}0)} = 6.5\ \text{J/m}^2$ [15].

Calculations established the regions that are most dangerous from the viewpoint of the brittle fracture of anvils during loading – under the unsupported hole and near the working surface (Fig. 4). It should be emphasized that during unloading there is one other likely fracture region – directly on the working surface [22]. One prerequisite for the formation of this region is a decrease in maximum lateral pressure to zero. It should be noted that the values of corrected equivalent stress $\sigma_e/\sigma^0_{(110)}$ shown in Fig. 4 were obtained with the assumption that m = 3.175. However, the value of m may change appreciably from crystal to crystal. Since the character of the pressure distribution and the shape of the anvils in the experiments in [9] were similar to the case we considered in our calculations (Figs. 1 and 2), we made an estimate of m to characterize anvil strength. With the assumption that fracture occurs at $\sigma_e/\sigma^0_{(110)}$, m should be equal to 6.35 GPa.

To optimize the geometry and loading conditions for diamond anvils, we decided to use approximate mathematical models obtained from analysis of the results of a numerical experiment in which the strength of such anvils was evaluated. An analysis of the range of service loads and variation of the geometric dimensions made it possible to find several characteristic patterns. A factorial experiment [23] was then performed. Due to the narrow range of variation of the factors being considered, we first assumed that the dependence of the strength of an anvil in the most heavily stressed regions on the anvil's geometry and loading conditions is described by a linear combination of n_i-th-degree polynomials of each i-th independent factor, i.e. we constructed a regression model to describe the principal effects. (A preliminary analysis established that the dependence of the stresses σ_e in the most heavily stressed regions on the dimensions of the anvil is expressed by a polynomial – Fig. 5):

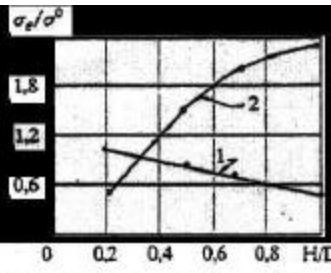

Fig. 5. Change in the corrected $\sigma_e/\sigma^0_{(110)}$ equivalent stresses in diamond anvils for different H/D in the region under the unsupported hole (1) and near the working surface of the anvils (2).

$$\sigma_e = b_0 + \sum_{i=1}^{k} \sum_{j=1}^{n_i} b_{ij} \varphi_{ij}(x_i),$$

where b_0 is the absolute term of the equation (the mean of σ_e within the given region); b_{ij} is the regression coefficient for the j-th-degree polynomial of the i-th factor; $\varphi_{ij}(x_i)$ is a j-th-degree polynomial of factor x_i; k is the number of factors examined; n_i is the maximum degree of polynomial for the i-th factor.

Recursion formulas were used to construct a system of orthogonal polynomials for each factor [24]:

$$\varphi_0 = 1;\ \varphi_1 = (x + a_1)\cdot\varphi_0;\ \ \varphi_\nu = (x + a_\nu)\cdot\varphi_{\nu-1} + b_\nu\cdot\varphi_{\nu-2},$$

where φ_ν is a polynomial of degree ν; a_ν and b_ν are coefficients. The experiment plan was chosen from the factorial experiment catalog [23] on the basis of the number of variables and the presumed degree of the polynomial. Each experiment involved a finite-element calculation of σ_e in the most heavily stressed regions. The number of each experiment was assigned in a matrix combining the dimensions and conditions of loading of diamond anvils.

The results of the experiments were analyzed with a set of programs [25] in order to obtain estimates of the regression coefficients and the errors of the approximation. If the model obtained to describe the principal effects provided satisfactorily accurate estimates of σ_e, we used it to then solve the optimization problem. Otherwise, we performed an additional analysis of the experimental data by automatically generating structural models in which there were two or three mutual effects between the given variables. We took this set of models and chose those which yielded satisfactory values of the response function at the different points of the experiment plan. The final selection of the approximating equation (from the chosen group) was made by comparing their accuracy in calculations of σ_e at intermediate (relative to the plan) points of the factor space.

The geometry and loading conditions for diamond anvils were optimized by searching for points of the factor space where the resulting model had a minimum. This problem was solved by the simplex method developed by Nelder and Mead. Here, the form of the simplex being displaced is adapted to the form of the response surface, and the number of iterations is reduced by selecting the proper displacement strategy. To search for the global minimum, the problem is solved repeatedly by constructing the initial simplex at different points uniformly distributed in the factor space with the aid of a random number generator.

For each characteristic configuration, we constructed mathematical models describing (to within 10%) the dependence of the strength of the anvils in the most heavily stressed region on their geometry and loading conditions. We examined the following ranges of the factors that were optimized (Fig. 6): D = 2.5-3.5 mm; D_1 = 2.5-4.55 mm; D_2 = 0.8-2.0 mm; d_1 = 0.01-0.18 mm; d_2 = 0.2-0.91 mm; h = 0.54-5.4 mm; h_1 = 0.05-0.805 mm; α = 0-20°; θ_1 = 30-65°; l = 0.02-0.5 mm. The dependence of strength on these factors was found in the form $\sigma_e/\sigma_{(110)}{}^0 = f(x_i)$, where x_i, i = 1, k. Thus, for example, we have the following for the region under the hole

$$\sigma_e \approx \frac{P_{\text{inc}}}{D_1^2 - D_2^2} \exp[b_0 + b_{11}\varphi_{11} + b_{12}\varphi_{12} + b_{21}\varphi_{21} + b_{22}\varphi_{22} + b_{31}\varphi_{31} + b_{32}\varphi_{32} +$$

$$+ b_{33}\varphi_{33} + b_{41}\varphi_{41} + b_{42}\varphi_{42} + b_{43}\varphi_{43} + b\tilde{b}_{11}\varphi_{11}\varphi_{41} + b\tilde{b}_{22}\varphi_{12}\varphi_{33} + b\tilde{b}_{23}\varphi_{23}\varphi_{41}],$$

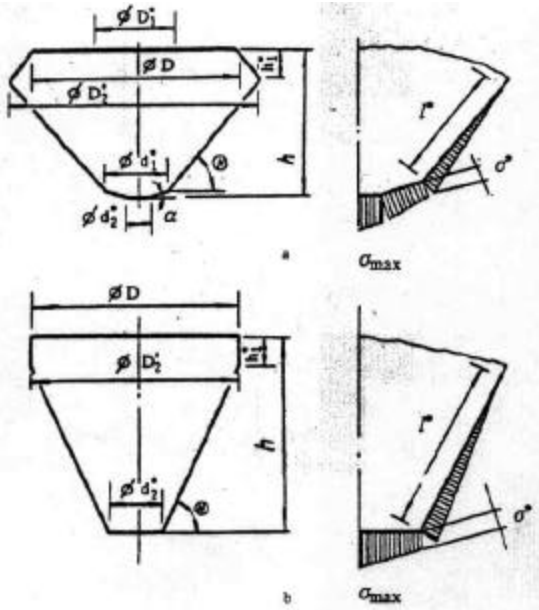

Fig. 6. Configuration of a diamond anvil and conditions of its loading that permit the attainment of theoretical pressures of 465 (a) and 435 GPa (b) ($D_1^* = D_1/D$; $D_2^* = D_2/D$; $h_1^* = h_1 = h_1/D$; $d_1^* = d_1/D$; $d_2^* = d_2/D$; $l^* = l/D$; $\sigma^* = \sigma'/\sigma_{max}$): a) D = 3.8 mm, h = 2.2 mm, $\sigma = 29°$, $\theta_1 = 40°$, $D_1^* = 0.39$, $D_2^* = 1.16$, $h_1^* = 0.146$, $d_1^* = 0.74$, $d_2^* = 0.015$, $l^* = 0.086$, $\sigma^* = 0.131$; b) D = 3.0 mm, h = 3.01 mm, $\sigma = 0°$, $\theta_1 = 65°$, $D_1^* = 0.6666$ (and $D_1^* = 0$), $D_2 = 1.0$, $h_1^* = 0.02$, $d_1^* = 0.08$, $d_2^* = 0.07$, $l^* = 0.2$, $\sigma^* = 0.165$.

where

$$\varphi_{11} = 100\frac{h_1}{D_1} - 13{,}5;\ \varphi_{12} = (100\frac{h_1}{D_1} - 13{,}5)\varphi_{11} - 73{,}46;$$

$$\varphi_{21} = 10\frac{h}{D_1} - 8{,}47;\ \varphi_{22} = (10\frac{h}{D_1} - 8{,}47)\varphi_{21} - 13{,}16;$$

$$\varphi_{23} = (10\frac{h}{D_1} - 8{,}47)\varphi_{22} - 8{,}42\varphi_{21};\ \varphi_{31} = \frac{D_2}{D_1} - 1{,}15;$$

$$\varphi_{32} = \left(\frac{D_2}{D_1} - 1{,}15\right)\varphi_{31} - 0{,}0125;\ \varphi_{33} = \left(\frac{D_2}{D_1} - 1{,}15\right)\varphi_{32} - 0{,}008\varphi_{31};$$

$$\varphi_{41} = 10\frac{D_2}{D_1} - 3{,}33;\ \varphi_{42} = \left(10\frac{D_2}{D_1} - 3{,}33\right)\varphi_{41} - 6{,}17;$$

$$\varphi_{43} = \left(10\frac{D_2}{D_1} - 3{,}33\right)\varphi_{42} - 3{,}95\varphi_{41};$$

$$P_{int} = \frac{\pi}{3}\left[\left(\frac{q_{max}}{2} + q_l\right)\frac{d_1^2}{2} + \left(\frac{d_1}{2} - \frac{d_1}{2}\right)\cdot\left[q_l\left(d_1 + \frac{d_2}{2}\right) + q_k\left(d_2 + \frac{d_1}{2}\right)\right] + \right.$$

$$\left. + l\cos\theta_1 q_k\left(3\frac{d_2}{2} + l\cos\theta_1\right)\right];$$

$b_0 = -0.1715$; $b_{11} = -0.0114$; $b_{12} = 0.0003$; $b_{21} = -0.2117$; $b_{22} = 0.026$; $b_{31} = -0.347$; $b_{32} = 2.853$; $b_{33} = 24.88$; $b_{41} = 0.097$; $b_{42} = -0.062$; $b_{43} = 0.018$; $bb_1 = -0.00096$; $bb_2 = -0.194$; $bb_3 = -0.00034$; q_{max}, q_j, q_k are the normal components of pressure along the anvil–interlayer contact line at $r = 0$, $r = d_1/2$, $r = d_2/2$, respectively; P_{int} is the integral force acting on the anvil. (In accordance with Saint-Venant's principle, the stresses away from the site of load application are independent of the character of load distribution and depend only on the integral force – as has been confirmed experimentally). Similar relations were found for each characteristic structure in regions of possible brittle fracture.

Our search for optimum points of the models that were constructed yielded combinations of optimized parameters that made it possible to attain theoretical pressures of 465 and 435 GPa (Fig. 6). It should be noted that these values were obtained with the assumption of a linear law [9] for pressure distribution over the working surface of the anvil when $m = 6.35$. Thus, the optimization established a combination of parameters that allow the pressure achieved previously to be exceeded by a factor of more than 2.5.

The use of materials with a greater angle of internal friction for the interlayer has made it possible to experimentally achieve pressures of roughly 550 GPa [26]. The character of pressure distribution over the working surface of the anvil for this case differs markedly from the linearity seen in [9] – a fact that will be considered in future refinements of the method presented here.

The method we have described for optimizing the structural parameters and loading conditions of diamond anvils and the results that have been obtained can be employed in the design of equipment using such anvils.

LITERATURE CITED

1. A. Jayaraman, "Ultrahigh pressure," Rev. Sci. Instrum., 57, No. 6, 1013-1031 (1986).
2. F. P. Bundy, "Design and development of apparatus to achieve the highest possible static pressures," Physica, 139, No. 140B, 42-51 (1986).
3. D. M. Adams and A. C. Shaw, "A computer-aided design study of the behavior of diamond anvil under stress," J. Phys. D: Appl. Phys., 15, No. 6, 1609-1635 (1982).
4. M. S. Bruno and K. J. Dunn, "Stress analysis of a beveled diamond anvil," Rev. Sci. Instrum., 55, No. 6, 940-943 (1984).
5. M. V. Astrakhan', B. I. Beresnev, and V. G. Synkov, "Design of diamond anvils," Sverkhtverdye Mater., No. 3, 16-20 (1986).
6. A. L. Ruoff, H. Xia, H. Luo, and Y. K. Vohra, "Miniaturization techniques for obtaining static pressures comparable to that at the center of the Earth: x-ray diffraction at 416 GPa," Rev. Sci. Instrum., 61, 9830 (1990).
7. A. L. Ruoff and H. Luo, Stresses and Strains in Diamond Anvils in the Multimegabar Range. To be published.
8. W. C. Moss and K. Goettel, "Finite element design of diamond anvils," Appl. Phys. Lett., 50, No. 1, 25-27 (1987).
9. H. K. Mao and P. M. Bell, "High-pressure: Sustained static generation of 1.36 to 1.72 Mbar," Science, 200, No. 4346, 1145-1147 (1978).
10. E. P. Unksov, Engineering Theory of Plasticity [in Russian], Mashgiz, Moscow (1959).
11. V. I. Levitas, Large Elastoplastic Strains of Materials at High Pressure [in Russian], Naukova Dumka, Kiev (1987).
12. V. V. Sokolovskii, Theory of Plasticity [in Russian], Vysshaya Shkola, Moscow (1969).
13. A. D. Platonov, "Optimization of finite-element methods for calculating parameters of linear fracture mechanics (K_1, K_2, J)," Author's Abstract of Engineering Sciences Candidate Dissertation, Kiev (1984).
14. N. V. Novikov, V. I. Levitas, R. A. Zolotarev, et al., "Testing of sets of programs developed to solve problems of thermomechanics," Dopov. Akad. Nauk Ukr. RSR, No. 4, 30-33 (1985).
15. J. E. Field, The Properties of Diamond, Academic Press, London, New York–San Francisco (1979).
16. S. G. Lekhnitskii, Theory of Elasticity of Anisotropic Bodies [in Russian], Nauka, Moscow (1977).
17. V. I. Levitas, "Construction of a theory of ideal plasticity," Probl. Prochn., No. 11, 56-62 (1980).
18. V. I. Levitas, "Certain models of the inelastic deformation of materials. Reports Nos. 1-2," ibid., No. 12, 70-83 (1980).

19. G. A. Voronin, V. I. Mal'nev, and G. F. Nevstruev, "Effect of inclusions on the strength of synthetic diamonds at high pressures," Sverkhtverdye Mater., No. 2, 33-37 (1984).
20. G. Libovitz (ed.), Fracture: Mathematical Principles of the Theory of Fracture [Russian translation], Mir, Moscow (1975), Vol. 2.
21. W. D. Harkins, "Energy relations of surface of solids," J. Chem. Phys., **10**, No. 5, 268 (1942).
22. S. B. Polotnyak, "Stress–strain state and limiting state of diamond anvils in a high-pressure apparatus during loading and unloading," in: Ultrahard Materials in the National Economy [in Russian], In-t Sverkhtverdykh Materialov, Kiev (1989), pp. 16-19.
23. F. S. Novik and Ya. B. Arsov, Use of Factorial Experiments to Optimize Metallurgical Processes [in Russian], Mashinostroenie, Moscow; Tekhnika, Sofia.
24. L. P. Ruzinov and R. I. Slobodchikova, Experiment Planning in Chemistry and Chemical Engineering [in Russian], Khimiya, Moscow (1980).
25. M. M. Potemkin, "Use of computers to study processes in the corrosion protection of metals," Materials of the Second All-Republic Scientific–Technical Conference on the Corrosion and Corrosion-Protection of Metals. "Development and Use of Anti-Corrosive Metallic Coatings," Summary of Documents, Dnepropetrovsk (1981), pp. 202-203.
26. J. A. Xu, H. K. Mao, and P. M. Bell, "High-pressure ruby and diamond fluorescence observation at 0.21 to 0.55 terapascal," Science, **232**, No. 4756 (1986), pp. 1404-1406.